

Differential cross section measurement of charged current ν_e interactions without final-state pions in MicroBooNE: Supplementary Material

P. Abratenko,³⁴ J. Anthony,⁴ L. Arellano,¹⁹ J. Asaadi,³³ A. Ashkenazi,³¹ S. Balasubramanian,¹¹ B. Baller,¹¹ C. Barnes,²¹ G. Barr,²⁴ J. Barrow,^{20,31} V. Basque,¹¹ L. Bathe-Peters,¹³ O. Benevides Rodrigues,³⁰ S. Berkman,¹¹ A. Bhanderi,¹⁹ M. Bhattacharya,¹¹ M. Bishai,² A. Blake,¹⁶ B. Bogart,²¹ T. Bolton,¹⁵ J. Y. Book,¹³ L. Camilleri,⁹ D. Caratelli,³ I. Caro Terrazas,⁸ F. Cavanna,¹¹ G. Cerati,¹¹ Y. Chen,²⁷ J. M. Conrad,²⁰ M. Convery,²⁷ L. Cooper-Troendle,³⁷ J. I. Crespo-Anadón,⁵ M. Del Tutto,¹¹ S. R. Dennis,⁴ P. Detje,⁴ A. Devitt,¹⁶ R. Diurba,^{1,22} R. Dorrill,¹⁴ K. Duffy,²⁴ S. Dytman,²⁵ B. Eberly,²⁹ A. Ereditato,¹ J. J. Evans,¹⁹ R. Fine,¹⁷ O. G. Finnerud,¹⁹ W. Foreman,¹⁴ B. T. Fleming,³⁷ N. Foppiani,¹³ D. Franco,³⁷ A. P. Furmanski,²² D. Garcia-Gamez,¹² S. Gardiner,¹¹ G. Ge,⁹ S. Gollapinni,^{32,17} O. Goodwin,¹⁹ E. Gramellini,¹¹ P. Green,¹⁹ H. Greenlee,¹¹ W. Gu,² R. Guenette,¹⁹ P. Guzowski,¹⁹ L. Hagaman,³⁷ O. Hen,²⁰ R. Hicks,¹⁷ C. Hilgenberg,²² G. A. Horton-Smith,¹⁵ B. Irwin,²² R. Itay,²⁷ C. James,¹¹ X. Ji,² L. Jiang,³⁵ J. H. Jo,³⁷ R. A. Johnson,⁷ Y.-J. Jwa,⁹ D. Kalra,⁹ N. Kamp,²⁰ G. Karagiorgi,⁹ W. Ketchum,¹¹ M. Kirby,¹¹ T. Kobilarcik,¹¹ I. Kreslo,¹ M. B. Leibovitch,³ I. Lepetic,²⁶ J.-Y. Li,¹⁰ K. Li,³⁷ Y. Li,² K. Lin,²⁶ B. R. Littlejohn,¹⁴ W. C. Louis,¹⁷ X. Luo,³ K. Manivannan,³⁰ C. Mariani,³⁵ D. Marsden,¹⁹ J. Marshall,³⁶ D. A. Martinez Caicedo,²⁸ K. Mason,³⁴ A. Mastbaum,²⁶ N. McConkey,¹⁹ V. Meddage,¹⁵ K. Miller,⁶ J. Mills,³⁴ A. Mogan,⁸ T. Mohayai,¹¹ M. Mooney,⁸ A. F. Moor,⁴ C. D. Moore,¹¹ L. Mora Lepin,¹⁹ J. Mousseau,²¹ S. Mullerababu,¹ D. Naples,²⁵ A. Navrer-Agasson,¹⁹ N. Nayak,² M. Nebot-Guinot,¹⁰ D. A. Newmark,¹⁷ J. Nowak,¹⁶ M. Nunes,³⁰ N. Oza,¹⁷ O. Palamara,¹¹ N. Pallat,²² V. Paolone,²⁵ A. Papadopoulou,²⁰ V. Papavassiliou,²³ H. B. Parkinson,¹⁰ S. F. Pate,²³ N. Patel,¹⁶ Z. Pavlovic,¹¹ E. Piaseczky,³¹ I. D. Ponce-Pinto,³⁷ S. Prince,¹³ X. Qian,² J. L. Raaf,¹¹ V. Radeka,² M. Reggiani-Guzzo,¹⁹ L. Ren,²³ L. Rochester,²⁷ J. Rodriguez Rondon,²⁸ M. Rosenberg,³⁴ M. Ross-Lonergan,^{9,17} C. Rudolf von Rohr,¹ G. Scanavini,³⁷ D. W. Schmitz,⁶ A. Schukraft,¹¹ W. Seligman,⁹ M. H. Shaevitz,⁹ R. Sharankova,¹¹ J. Shi,⁴ A. Smith,⁴ E. L. Snider,¹¹ M. Soderberg,³⁰ S. Söldner-Rembold,¹⁹ J. Spitz,²¹ M. Stancari,¹¹ J. St. John,¹¹ T. Strauss,¹¹ S. Sword-Fehlberg,²³ A. M. Szelc,¹⁰ W. Tang,³² N. Taniuchi,⁴ K. Terao,²⁷ C. Thorpe,¹⁶ D. Torbunov,² D. Totani,³ M. Toups,¹¹ Y.-T. Tsai,²⁷ J. Tyler,¹⁵ M. A. Uchida,⁴ T. Usher,²⁷ B. Viren,² M. Weber,¹ H. Wei,¹⁸ A. J. White,³⁷ Z. Williams,³³ S. Wolbers,¹¹ T. Wongjirad,³⁴ M. Wospakrik,¹¹ K. Wresilo,⁴ N. Wright,²⁰ W. Wu,¹¹ E. Yandel,³ T. Yang,¹¹ L. E. Yates,¹¹ H. W. Yu,² G. P. Zeller,¹¹ J. Zennamo,¹¹ and C. Zhang²

(The MicroBooNE Collaboration)*

¹Universität Bern, Bern CH-3012, Switzerland

²Brookhaven National Laboratory (BNL), Upton, NY, 11973, USA

³University of California, Santa Barbara, CA, 93106, USA

⁴University of Cambridge, Cambridge CB3 0HE, United Kingdom

⁵Centro de Investigaciones Energéticas, Medioambientales y Tecnológicas (CIEMAT), Madrid E-28040, Spain

⁶University of Chicago, Chicago, IL, 60637, USA

⁷University of Cincinnati, Cincinnati, OH, 45221, USA

⁸Colorado State University, Fort Collins, CO, 80523, USA

⁹Columbia University, New York, NY, 10027, USA

¹⁰University of Edinburgh, Edinburgh EH9 3FD, United Kingdom

¹¹Fermi National Accelerator Laboratory (FNAL), Batavia, IL 60510, USA

¹²Universidad de Granada, Granada E-18071, Spain

¹³Harvard University, Cambridge, MA 02138, USA

¹⁴Illinois Institute of Technology (IIT), Chicago, IL 60616, USA

¹⁵Kansas State University (KSU), Manhattan, KS, 66506, USA

¹⁶Lancaster University, Lancaster LA1 4YW, United Kingdom

¹⁷Los Alamos National Laboratory (LANL), Los Alamos, NM, 87545, USA

¹⁸Louisiana State University, Baton Rouge, LA, 70803, USA

¹⁹The University of Manchester, Manchester M13 9PL, United Kingdom

²⁰Massachusetts Institute of Technology (MIT), Cambridge, MA, 02139, USA

²¹University of Michigan, Ann Arbor, MI, 48109, USA

²²University of Minnesota, Minneapolis, MN, 55455, USA

²³New Mexico State University (NMSU), Las Cruces, NM, 88003, USA

²⁴University of Oxford, Oxford OX1 3RH, United Kingdom

²⁵University of Pittsburgh, Pittsburgh, PA, 15260, USA

²⁶Rutgers University, Piscataway, NJ, 08854, USA

²⁷SLAC National Accelerator Laboratory, Menlo Park, CA, 94025, USA

²⁸South Dakota School of Mines and Technology (SDSMT), Rapid City, SD, 57701, USA

²⁹University of Southern Maine, Portland, ME, 04104, USA

³⁰*Syracuse University, Syracuse, NY, 13244, USA*

³¹*Tel Aviv University, Tel Aviv, Israel, 69978*

³²*University of Tennessee, Knoxville, TN, 37996, USA*

³³*University of Texas, Arlington, TX, 76019, USA*

³⁴*Tufts University, Medford, MA, 02155, USA*

³⁵*Center for Neutrino Physics, Virginia Tech, Blacksburg, VA, 24061, USA*

³⁶*University of Warwick, Coventry CV4 7AL, United Kingdom*

³⁷*Wright Laboratory, Department of Physics, Yale University, New Haven, CT, 06520, USA*

(Dated: August 3, 2022)

I. PROTON THRESHOLD

The choice of the proton threshold at 50 MeV is motivated by Fig. 1, where we show the expected number of selected signal events as a function of the true leading proton kinetic energy for the $1e0p0\pi$ and $1eNp0\pi$ selections. The choice of 50 MeV corresponds to the energy where the two curves intersect, so below this value most events are selected with the $1e0p0\pi$ selection, while above this value most events are selected with the $1eNp0\pi$ selection.

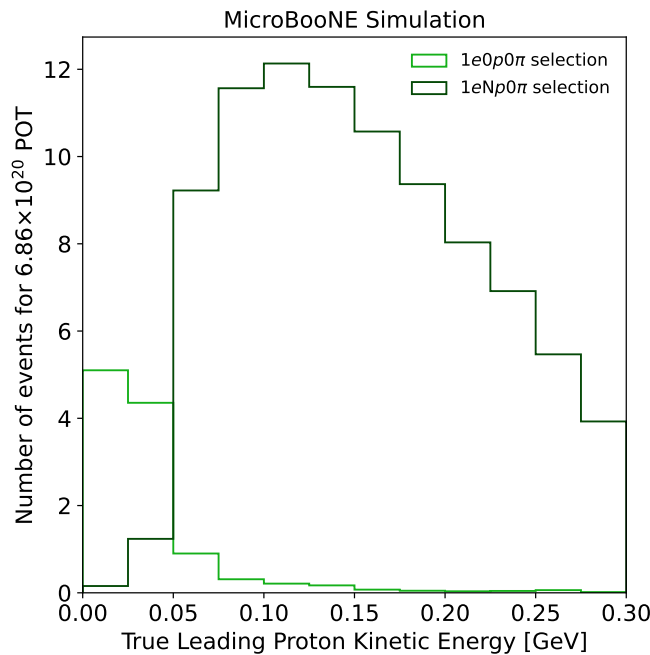


FIG. 1. Expected number of signal events for 6.86×10^{20} POT as a function of the leading proton kinetic energy for the $1e0p0\pi$ and $1eNp0\pi$ selections.

* microboone.info@fnal.gov

II. INTERACTION MODE OF SELECTED EVENTS

In addition to true visible final state the selected neutrino events can also be classified by true interaction mode. The interaction mode breakdown for the tuned version of GENIE v3 is shown in Fig. 2 for events passing the cross-section selection in all four variables in which the cross section is measured.

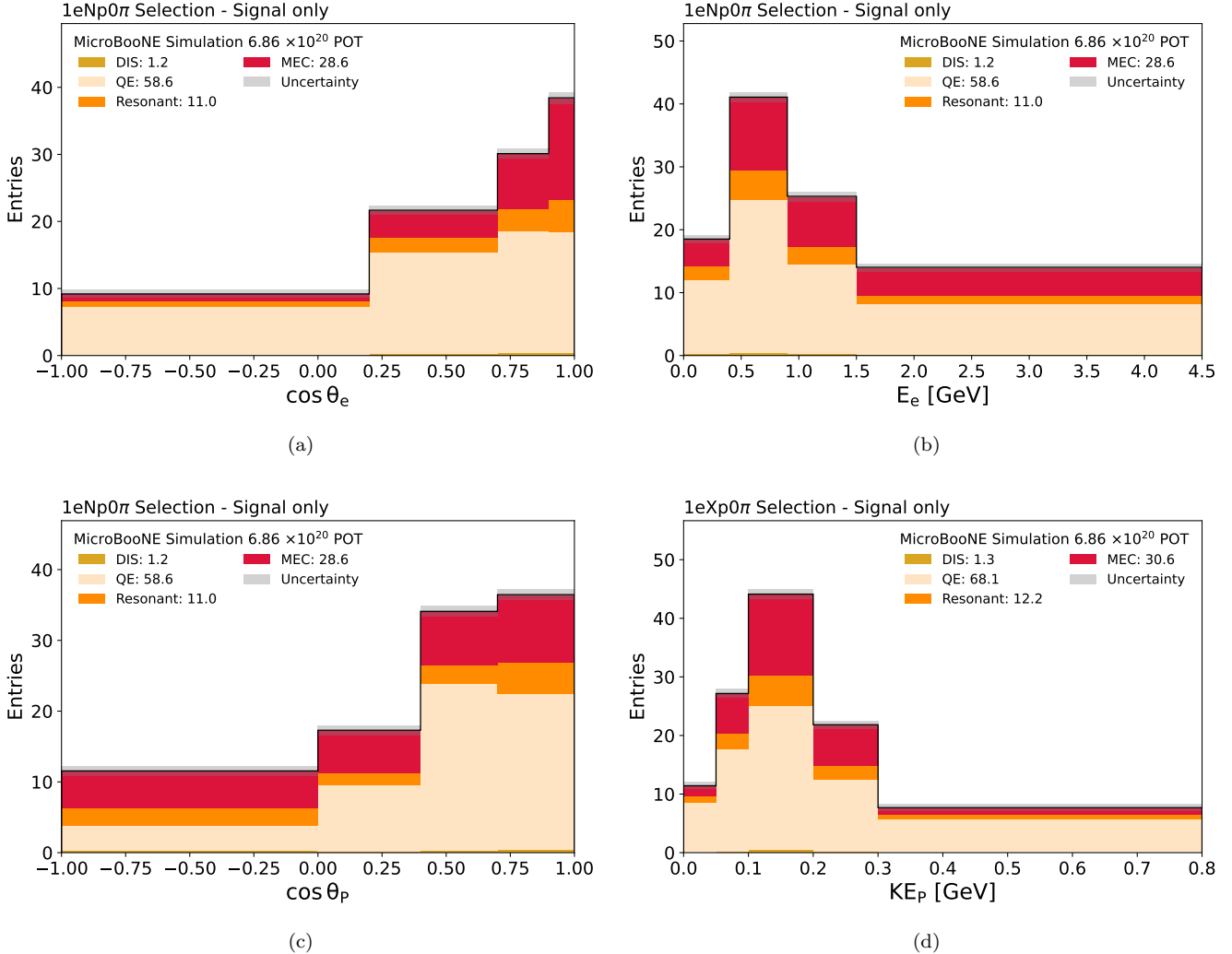


FIG. 2. Signal prediction using the MicroBooNE tune of GENIE v3 after selection, categorized by interaction mode: quasi-elastic (QE), meson exchange current (MEC), resonant, and deep inelastic scattering (DIS). The prediction is shown in (a) the angle between the neutrino beam and the electron direction, (b) electron kinetic energy, (c) the angle between the neutrino beam and the leading proton direction, and (d) the leading proton kinetic energy. The uncertainty band includes only statistical uncertainties of the simulated samples.

III. ELECTRON ENERGY

The tables in this section provide additional information for the cross-section measurement as a function of the electron energy: background-subtracted observation and cross-section values (Table I), χ^2 values for the different generators tests (Table II), covariance matrices for the extracted cross section (Table III) and for the background-subtracted data prediction (Table IV), and response matrix (Table V).

TABLE I. Unfolded cross section as a function of electron energy.

Bin [GeV]	[0, 0.4]	[0.4, 0.9]	[0.9, 1.5]	[1.5, 4.5]
Background-subtracted data events	11.86	21.75	15.11	14.80
Cross section [10^{-39} cm 2 /GeV/nucleon]	1.86	1.76	0.99	0.31

TABLE II. Results of compatibility tests between generators and the measured cross-section as a function of electron energy.

	GENIE v3 uB	GENIE v3	GENIE v2	NuWro	NEUT
χ^2	6.83	2.75	6.39	4.30	9.12
d.o.f.	4	4	4	4	4
p -value	0.145	0.600	0.172	0.367	0.058

TABLE III. Covariance matrix for the cross section measurement as a function of electron energy. Units are (cm 2 /GeV/nucleon) 2 .

Bin [GeV]	[0, 0.4]	[0.4, 0.9]	[0.9, 1.5]	[1.5, 4.5]
[0, 0.4]	2.46e-78	1.07e-79	-5.40e-81	8.67e-81
[0.4, 0.9]	1.07e-79	6.68e-79	2.04e-80	5.96e-82
[0.9, 1.5]	-5.40e-81	2.04e-80	2.60e-79	4.24e-82
[1.5, 4.5]	8.67e-81	5.96e-82	4.24e-82	1.21e-80

TABLE IV. Covariance matrix for the total event prediction as a function of electron energy.

Bin [GeV]	[0, 0.4]	[0.4, 0.9]	[0.9, 1.5]	[1.5, 4.5]
[0, 0.4]	63.99	13.57	4.59	2.44
[0.4, 0.9]	13.57	76.73	7.32	4.17
[0.9, 1.5]	4.59	7.32	44.73	3.07
[1.5, 4.5]	2.44	4.17	3.07	29.27

TABLE V. Response matrix for signal events as a function of electron energy.

Bin [GeV]	[0, 0.4]	[0.4, 0.9]	[0.9, 1.5]	[1.5, 4.5]
[0, 0.4]	0.097	0.026	0.003	0.001
[0.4, 0.9]	0.012	0.156	0.053	0.005
[0.9, 1.5]	0.000	0.010	0.144	0.040
[1.5, 4.5]	0.000	0.000	0.007	0.126

IV. ELECTRON ANGLE

The tables in this section provide additional information for the cross-section measurement as a function of the electron angle: background-subtracted observation and cross-section values (Table VI), χ^2 values for the different generators tests (Table VII), covariance matrices for the extracted cross section (Table VIII) and for the background-subtracted data prediction (Table IX), and response matrix (Table X).

TABLE VI. Unfolded cross section as a function of electron angle.

Bin	$[-1, 0.2]$	$[0.2, 0.7]$	$[0.7, 0.9]$	$[0.9, 1]$
Background-subtracted data events	5.96	13.73	17.98	27.20
Cross section [10^{-39} cm 2 /nucleon]	0.47	1.41	3.71	10.94

TABLE VII. Results of compatibility tests between generators and the measured cross-section as a function of electron angle.

	GENIE v3 uB	GENIE v3	GENIE v2	NuWro	NEUT
χ^2	4.67	0.95	4.70	2.14	6.56
d.o.f.	4	4	4	4	4
p -value	0.322	0.917	0.319	0.710	0.161

TABLE VIII. Covariance matrix for the cross section measurement as a function of electron angle. Units are (cm 2 /nucleon) 2 .

Bin	$[-1, 0.2]$	$[0.2, 0.7]$	$[0.7, 0.9]$	$[0.9, 1]$
$[-1, 0.2]$	1.99e-79	2.07e-80	8.05e-80	1.14e-79
$[0.2, 0.7]$	2.07e-80	4.81e-79	9.68e-80	2.29e-79
$[0.7, 0.9]$	8.05e-80	9.68e-80	2.82e-78	3.86e-79
$[0.9, 1]$	1.14e-79	2.29e-79	3.86e-79	1.26e-77

TABLE IX. Covariance matrix for the total event prediction as a function of electron angle.

Bin	$[-1, 0.2]$	$[0.2, 0.7]$	$[0.7, 0.9]$	$[0.9, 1]$
$[-1, 0.2]$	29.30	4.24	4.74	3.63
$[0.2, 0.7]$	4.24	41.05	8.05	5.83
$[0.7, 0.9]$	4.74	8.05	55.58	9.60
$[0.9, 1]$	3.63	5.83	9.60	73.74

TABLE X. Response matrix for signal events as a function of electron angle.

Bin	$[-1, 0.2]$	$[0.2, 0.7]$	$[0.7, 0.9]$	$[0.9, 1]$
$[-1, 0.2]$	0.084	0.003	0.000	0.000
$[0.2, 0.7]$	0.003	0.152	0.007	0.000
$[0.7, 0.9]$	0.000	0.009	0.182	0.008
$[0.9, 1]$	0.000	0.000	0.010	0.201

V. PROTON ENERGY

The tables in this section provide additional information for the cross-section measurement as a function of the proton kinetic energy: background-subtracted observation and cross-section values (Table XI), χ^2 values for the different generators tests (Table XII), covariance matrices for the extracted cross section (Table XIII) and for the background-subtracted data prediction (Table XIV), and response matrix (Table XV).

TABLE XI. Unfolded cross section as a function of proton energy.

Bin [GeV]	[0, 0.05]	[0.05, 0.1]	[0.1, 0.2]	[0.2, 0.3]	[0.3, 0.8]
Background-subtracted data events	7.81	13.20	35.03	10.72	7.30
Cross section [10^{-39} cm 2 /GeV/nucleon]	10.15	9.32	13.66	4.49	1.72

TABLE XII. Results of compatibility tests between generators and the measured cross-section as a function of proton energy.

	GENIE v3 uB	GENIE v3	GENIE v2	NuWro	NEUT
χ^2	6.35	2.41	7.53	2.73	6.85
d.o.f.	4	4	4	4	4
p -value	0.273	0.791	0.184	0.742	0.232

TABLE XIII. Covariance matrix for the cross section measurement as a function of proton energy. Units are (cm 2 /GeV/nucleon) 2 .

Bin [GeV]	[0, 0.05]	[0.05, 0.1]	[0.1, 0.2]	[0.2, 0.3]	[0.3, 0.8]
[0, 0.05]	5.64e-77	1.06e-78	1.95e-78	1.16e-78	1.79e-79
[0.05, 0.1]	1.06e-78	5.82e-77	2.95e-78	1.65e-78	2.55e-79
[0.1, 0.2]	1.95e-78	2.95e-78	1.46e-77	1.63e-79	5.19e-80
[0.2, 0.3]	1.16e-78	1.65e-78	1.63e-79	8.33e-78	9.57e-80
[0.3, 0.8]	1.70e-79	2.55e-79	5.19e-80	9.57e-80	7.11e-79

TABLE XIV. Covariance matrix for the total event prediction as a function of proton energy.

Bin [GeV]	[0, 0.05]	[0.05, 0.1]	[0.1, 0.2]	[0.2, 0.3]	[0.3, 0.8]
[0, 0.05]	25.79	4.83	5.87	2.28	0.68
[0.05, 0.1]	4.83	60.84	13.28	5.46	1.52
[0.1, 0.2]	5.87	13.28	85.58	7.69	2.20
[0.2, 0.3]	2.28	5.46	7.69	37.20	2.08
[0.3, 0.8]	0.68	1.52	2.20	2.08	13.31

TABLE XV. Response matrix for signal events as a function of proton energy.

Bin [GeV]	[0, 0.05]	[0.05, 0.1]	[0.1, 0.2]	[0.2, 0.3]	[0.3, 0.8]
[0, 0.05]	0.108	0.009	0.003	0.001	0.001
[0.05, 0.1]	0.015	0.150	0.024	0.008	0.002
[0.1, 0.2]	0.001	0.006	0.192	0.036	0.006
[0.2, 0.3]	0.000	0.000	0.003	0.163	0.018
[0.3, 0.8]	0.000	0.000	0.000	0.001	0.068

VI. PROTON ANGLE

The tables in this section provide additional information for the cross-section measurement as a function of the proton angle: background-subtracted observation and cross-section values (Table XVI), χ^2 values for the different generators tests (Table XVII), covariance matrices for the extracted cross section (Table XVIII) and for the background-subtracted data prediction (Table XIX), and response matrix (Table XX).

TABLE XVI. Unfolded cross section as a function of proton angle.

Bin	$[-1, 0]$	$[0, 0.4]$	$[0.4, 0.7]$	$[0.7, 1]$
Background subtracted data events	7.09	23.80	16.74	17.22
Cross section [10^{-39} cm 2 /nucleon]	0.26	2.88	2.14	3.25

TABLE XVII. Results of compatibility tests between generators and the measured cross-section as a function of proton angle.

	GENIE v3 uB	GENIE v3	GENIE v2	NuWro	NEUT
χ^2	11.86	8.63	12.64	9.98	14.55
d.o.f.	4	4	4	4	4
p -value	0.018	0.071	0.013	0.041	0.006

TABLE XVIII. Covariance matrix for the cross section measurement as a function of proton angle. Units are (cm 2 /nucleon) 2 .

Bin	$[-1, 0]$	$[0, 0.4]$	$[0.4, 0.7]$	$[0.7, 1]$
$[-1, 0]$	7.69e-80	1.02e-80	1.11e-80	5.50e-80
$[0, 0.4]$	1.02e-80	4.51e-79	-1.89e-80	6.47e-80
$[0.4, 0.7]$	1.11e-80	-1.89e-80	1.15e-78	1.25e-79
$[0.7, 1]$	5.50e-80	6.47e-80	1.25e-79	3.88e-78

TABLE XIX. Covariance matrix for the total event prediction as a function of proton angle.

Bin	$[-1, 0]$	$[0, 0.4]$	$[0.4, 0.7]$	$[0.7, 1]$
$[-1, 0]$	29.52	3.02	3.80	8.21
$[0, 0.4]$	3.02	28.10	3.93	6.81
$[0.4, 0.7]$	3.80	3.93	52.33	10.99
$[0.7, 1]$	8.21	6.81	10.99	86.76

TABLE XX. Response matrix for signal events as a function of proton angle.

Bin	$[-1, 0]$	$[0, 0.4]$	$[0.4, 0.7]$	$[0.7, 1]$
$[-1, 0]$	0.140	0.016	0.005	0.005
$[0, 0.4]$	0.011	0.152	0.014	0.003
$[0.4, 0.7]$	0.006	0.019	0.175	0.010
$[0.7, 1]$	0.009	0.005	0.017	0.126